V Physics Summer Program, Mainz-Valencia

In the Search of the Decay $K_S^0 \to \mu^+\mu^-\gamma$

Pérez Díaz, Pablo José

September, 2002

Abstract

Our object is to find the decay $K_S^0 \to \mu^+\mu^-\gamma$, study the cuts we can make to remove background, and if possible calculate the branching fraction of this particular channel.

1 Neutral Kaons

Hadrons are built by the associaton of quarks, and when two quarks associate we say that it is a Meson. Kaons are one kind of mesons with some particular quarks, and there are several types of them. One of the first divisions we can make is between the ones that have charge ($K^\pm$) and the ones that are neutral (K^0), which we are interested in. K^0 is composed by a $\bar{s}$ quark and d quark, while its antiparticle $\bar{K}^0$ is made by an s quark and $\bar{d}$ quark.

These two particles are only eigenstates of the strong interaction, but not of the combined operation CP[1]. However, a mixture of them can be a CP eigenstate, thus we get the states K_1 and K_2:

$$K_1 = \frac{1}{\sqrt{2}}\Big(|K^0\rangle + |\bar{K}^0\rangle\Big)(CP = +1)$$

[1] $CP|K^0\rangle = |\bar{K}^0\rangle$

$$K_2 = \frac{1}{\sqrt{2}}\Big(|K^0\rangle - |\bar{K}^0\rangle\Big)(CP = -1)$$

But we cannot observe directly in nature K_1 and K_2, instead we observe two kinds of neutral kaons, ones that live very long, and others that have much less mean lifetime, we call these physical states K_L^0 and K_S^0.

To have CP conserved, as the main decay channels of this particles are the pions, we have got that $K_1 \to \pi\pi$ and $K_2 \to \pi\pi\pi$. This second decay is much less probable than the first decay, because it leaves much less free energy, so it was thought that K_1 was K_S^0 and K_2 was K_L^0. However, it was found in 1964[1] that K_L^0 could also decay into two pions. This is mainly CP indirect violation by mixing procedures.

So we can try to build a combination of K_1 and K_2 to get the physical states of the kaons[2] (*mass eigenstates* are called) and it can be found that:

$$K_S^0 = \frac{1}{\sqrt{1+|\epsilon|^2}}\Big(|K_1\rangle + \epsilon|K_2\rangle\Big)$$

$$K_L^0 = \frac{1}{\sqrt{1+|\epsilon|^2}}\Big(\epsilon|K_1\rangle + |K_2\rangle\Big)$$

The difference between K_L^0 and K_S^0 are their lifetimes and the decay channels they have (see tables 1 and 2).

Table 1: $K_{L,S}$ Lifetime Comparison

	K_S	K_L
τ	$0.8935 \times 10^{-10} s$	$5.17 \times 10^{-8} s$
$c\tau$	2.6786 cm	15.51 m

2 $K_{L,S}^0$ Decays

K_L and K_S[3] mostly decay into the channels shown in table 2. My study in particular will be about $K_S^0 \to \mu^+\mu^-\gamma$, which is one of the possibilities of

[2] That is, K_L^0 and K_S^0

[3] We will suppose that we talk about neutral kaons and sometimes omit the ^{0}

the more general and unlikely[4] decay $K_{S,L} \to \gamma\gamma$, where each one of these gammas can be real or virtual. Processes leading to the production of real or virtual photons can be seen in the figures 1 and 2, and all the possible combinations of this decay are shown in table 3.

Table 2: $K^0_{L,S}$ Main Decay Channels

$K^0_S \to$	%	$K^0_L \to$	%
$\pi^+\pi^-$	68.61	$3\pi^0$	21.13
$\pi^0\pi^0$	31.39	$\pi^+\pi^-\pi^0$	12.55
$\pi^+\pi^-\gamma$	1.78×10^{-3}	$\pi^\pm\mu^\mp\nu_\mu(K^0_{\mu 3})$	27.18
		$\pi^\pm e^\mp\nu_e(K^0_{e3})$	38.78

Table 3: Two Photon Decay

$K_{S,L} \to$	
$\gamma\gamma$	both real photons
$e^+e^-\gamma$	$1 \times \gamma^{(*)} \to e^+e^-$
$\mu^+\mu^-\gamma$	$1 \times \gamma^{(*)} \to \mu^+\mu^-$
$e^+e^-e^+e^-$	$2 \times \gamma^{(*)} \to e^+e^-$
$\mu^+\mu^-\mu^+\mu^-$	$2 \times \gamma^{(*)} \to \mu^+\mu^-$
$\mu^+\mu^-e^+e^-$	$1 \times \gamma^{(*)} \to \mu^+\mu^- + 1 \times \gamma^{(*)} \to e^+e^-$

3 The NA48 Experiment

The NA48 Experiment is located at the CERN facilities in Geneva. It uses the Super Proton Synchrotron (SPS) to accelerate protons up to 400 GeV and make the colide to a 2 mm diameter, 400 mm long rod of beryllium. The intensity we get now is 5×10^{10} protons per burst[5].

[4]That is why most of them do not appear in the table
[5]Aprox. 5 seconds

Figure 1: $K \to \gamma\gamma$ Feynman Diagram

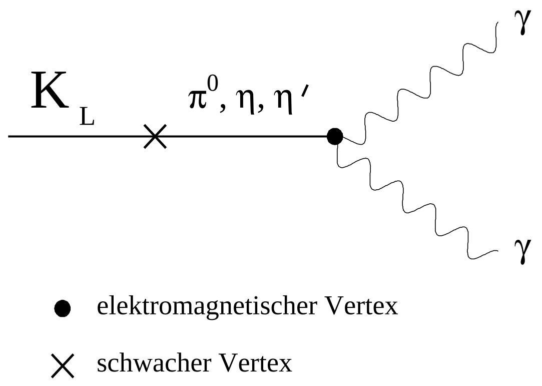

Downstream the target, the beam enters the field of a strong, vertical sweeping magnet, the gap of which is filled with tungsten-alloy inserts containing a passage for the neutral beam. This passage is shaped to absorb the remaining primary protons at a point where they are separated form the neutral beam, and to intercept the curved trajectories of all charged secondary particles from the target.

The magnet is followed by a steel collimator, which is fitted with further precisely-bored inserts, ranging from a beam defining aperture of 3.6 mm at

Figure 2: $K \to \gamma\gamma^*$ FEYNMAN DIAGRAM

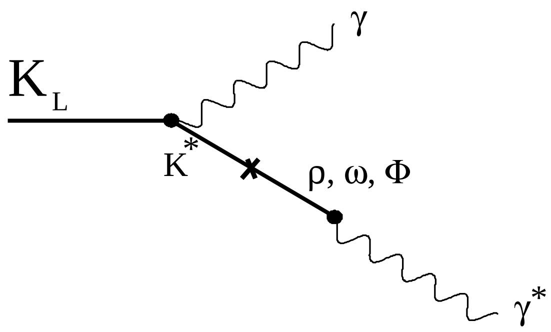

4.8 m from the target to a final diameter of 6.0 mm a the exit, 6.0 m after the target, where the K_S beam enters the decay volume. The overall length of the K_S collimator is close to 1 $c\tau_{K_S}$[2].

The main components of the detector consist of a high resolution liquid krypton calorimeter (LKr) and a magnetic spectrometer. To pre-trigger on charged decays, a plastic scintillator charged hodoscope (CHOD) is used. The hadron calorimeter is used to keep the pre-trigger rate low enough to strobe the Level II charged trigger and to also reconstruct hadronic energy.

A set of seven anti-counter rings (AKL) surrounding the vacuum decay tank is used to veto charged and neutral particles escaping from the fiducial region. A muon filter at the end of the hall provides a two-muon trigger.

Summarizing, with our experimental setup we can measure the momentum and energy of a track, the energy of neutral particles (that do not leave track) and we can also say if a track is from a muon or not. A picture of the detector can be seen in figure 3.

Figure 3: NA48 Experiment

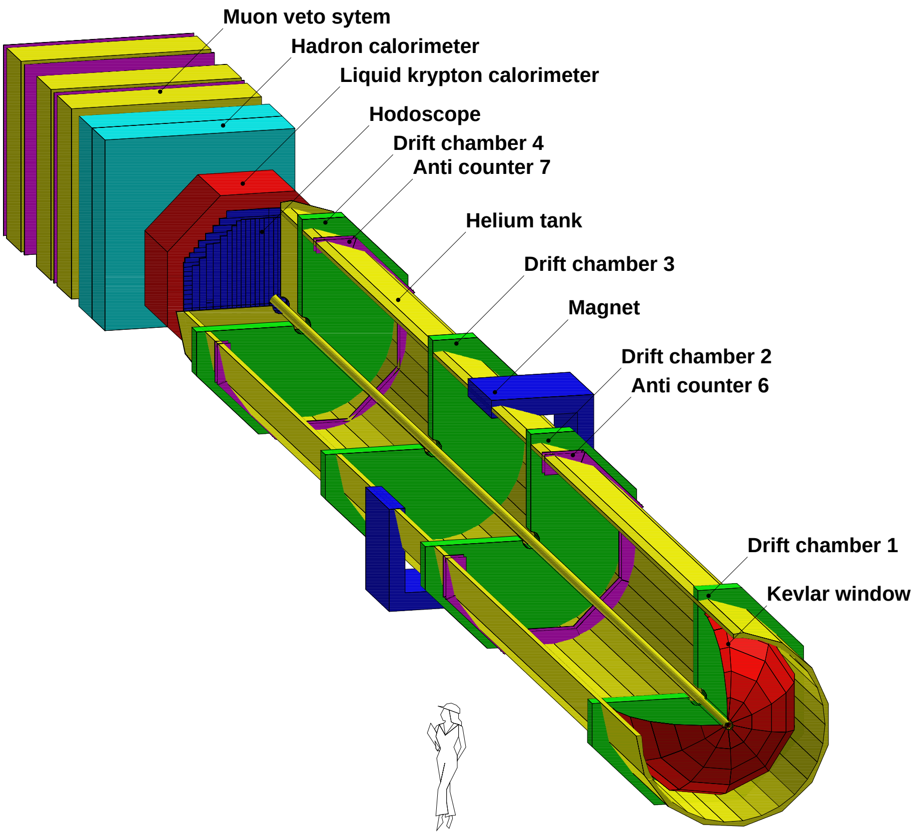

4 Background Sources

We have to deal with the background in our analysis. When the beam impacts the target several particles appear, and they can decay into many different channels. The most dangerous background is the most similar to our decay, that is a positive muon, a negative one and a photon. All the decays that can fit into this profile have to be removed.

Table 4: $K^0_{L,S}$ Important Background Sources

$K_S \to \pi^+\pi^-$	$K_S \to \pi^+\pi^-\gamma$
$K_L \to \pi^+\pi^-\pi^0$	$K_S \to \pi^\pm e^\mp \nu_e$
$K^0_{\mu 3}$	K^0_{e3}
$\Lambda \to p\pi^-$	$\Lambda \to p\pi^-\gamma$

- $K_S \to \pi^+\pi^-$ and $K_S \to \pi^+\pi^-\gamma$ decays. This two decays are really one[6]. The problem is that pions can decay to muon plus neutrino ($\pi \to \mu\nu$) and then this channel becomes very similar to a $\mu\mu\gamma$ decay. Also, the muon detector can misidentify one or two of the pions, and this effect added to the pion decay makes this background dangerous. We also have the photons, that in this case will come from bremsstrahlung.

- $K_L \to \pi^+\pi^-\pi^0$ The π^0 of this channel almost always decay inmediatly to $\gamma\gamma$, so we have the photon and the two tracks, but we lose the other photon, so when we build the $\mu\mu\gamma$ invariant mass it gives us a peak at 0.35 GeV. The pions have also to decay to muons or be misidentified.

- $K_{\mu 3}$ Here we already have a muon, and only one pion has to decay or be misidentified. However, there is no photon here, but it can be an accidental one (from other decay, for example).

- Λ *decays*. Due to the lifetime of Λ particle, which is very similar[7] to the K_S, we also have to deal with this background, but it is by far not the most important.

[6] It is usual to consider there is a photon only if it has a certain quantity of energy, because $K_S \to \pi^+\pi^-$ also emits low energy bremsstralung photons

[7] 2.632×10^{-10} s

5 Cuts Applied

5.1 Muon detector

In the final stage of our experimental setup we have a muon filter, which identifies whether if the track is a muon or not. As the two tracks that we have are muons, we will require in our analysis that the detector found a muon in the both tracks (of course, the detector is not perfect and we misidentify some).

5.2 Energy over Momentum

The spectrum of the ratio energy/momentum (see figure 4) in a track depends of the particle that leaves the track. In principle it should be around 1 for high energy particles[8] , but of course we do not detect all the energy of the track in our calorimeter. For example, muons interact very little with matter, and they go through the calorimeter without depositing any energy or very few, so we have very low E over P (Eop) ratio.

However, pions are so massive that they produce such a big shower of particles when they enter the calorimeter that part of the shower can remain undetected because it is outside the calorimeter. Pions will give us a very wide peak ranging from low values to 1.

We have also electrons, which produce small showers in our calorimeter, so we can get all the energy that it had; it will give us a peak around 1.

In our analysis we apply a cut that requires an $Eop < 0.1$ for an event to be counted. This is a very efective cut that removes all the electrons, and lots of pions also (but we have many, many pions).

5.3 Momenta of the Tracks

We require that the ratio of the momentum of the positive and the negative track must be less than 3. This cuts very little of our events, and removes most of the $\Lambda \to p\pi^-$ and $\Lambda \to p\pi^-\gamma$, because in this kind of events the momentum is taken mostly by the photon (see figure 5).

We also cut on the minimum (for high efficiency of the detector reasons) and maximum (to get rid of Λ decays) values of the momenta.

[8] $E = \sqrt{p^2 + m^2} \approx p$ if $p \gg m$

Figure 4: E over P Spectrum

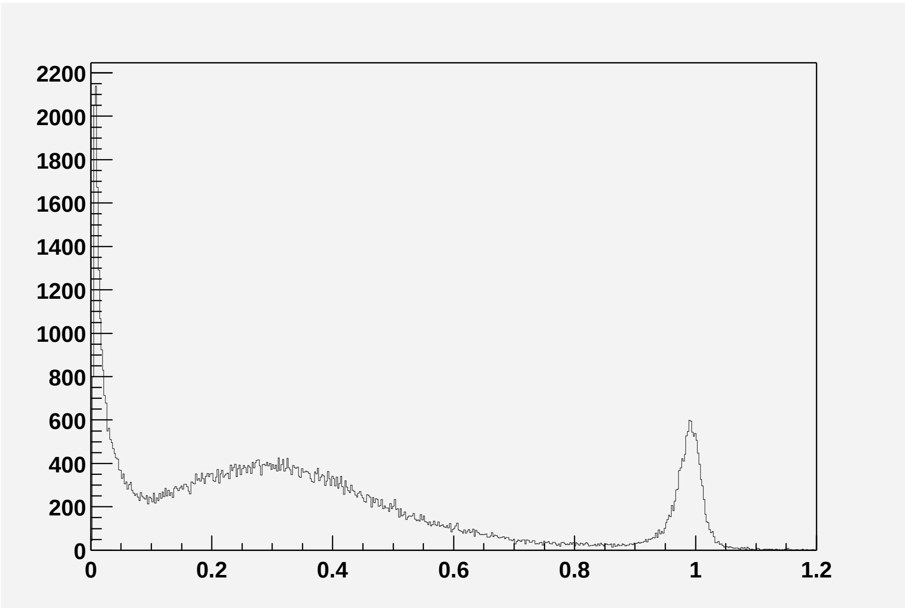

Figure 5: Ratio of Momenta of Positive and Negative Tracks

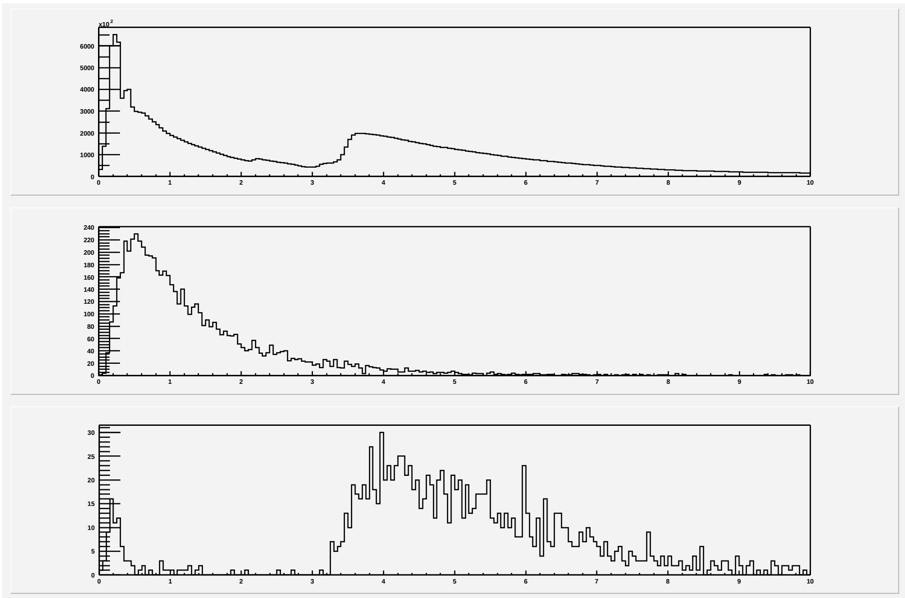

The upper histogram is real data, the middle one is data from $K_S \to \mu^+\mu^-\gamma$ Montecarlo, and the last is $\Lambda \to p\pi^-$ Montecarlo

5.4 Invariant Masses Cuts

We can select two tracks and a photon and build invariant masses for the biggest sources of background: $K \to \pi^+\pi^-$ and $K \to \pi^+\pi^-\gamma$. Then we will obtain a peak plus a flat distribution, and we delete the peak, which are the events corresponding to $K \to \pi^+\pi^-$ and $K \to \pi^+\pi^-\gamma$. This cuts lots of these events.

5.5 Existence of a Photon

In our decay we have a photon, and as it is a neutral particle, it leaves no track in the drift chambers: we only have the information of the clusters seen in the LKr for that event. What we do is extrapolate the position of the track in the LKr, and then look for clusters (showers) which are at more than 10 cm away from both tracks extrapolated positions.

Then we make a cut in the time of hit to eliminate the accidental photons from other decays, and we also cut on the energy of the photon found, because we have bremsstrahlung photons and they do not belong to our analysis. In figure 6 can be seen how effective this cut is. For example good cuts can be made at 10 GeV, but it is advisable to make them at 15 GeV, because our acceptance do not falls so much (table 5) and we delete a lot of background.

5.6 Transversal Momentum

This is a cut we use to identify missing products of decay. As we know the momenta of the two tracks and of the photon, we can build a total momentum of the sum of the decay products, and compare it with the direction of the kaon if it did not decay. If we had identified all the products of decay, in principle these two vectors should have the same direction, but if that decay had more products, the directions would not be the same.

The cut just consists in calculating the total momentum vector of the decay products and projecting it into the kaon direction, if it is too big we say that we missed some decay product, and that cannot be our reaction.

This cut is particularly good to surpress background coming from decaying pions, such as from $K_S \to \pi^+\pi^-\gamma \to \mu^+\nu\mu^-\bar{\nu}\gamma$. That is because the neutrinos remain undetected, while they take part of the momentum of the decaying pion, changing then the direction the muon detected.

Figure 6: ENERGY OF THE PHOTON FOUND

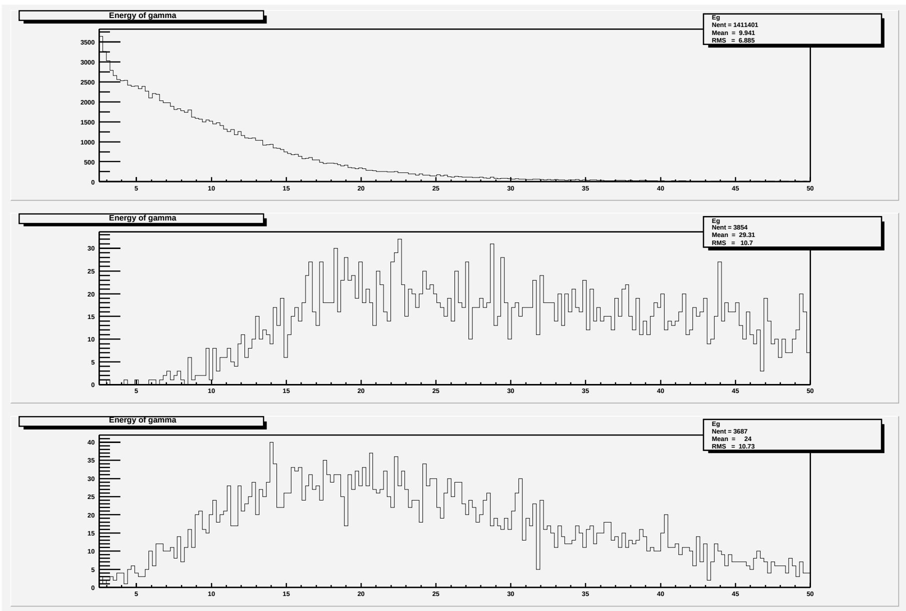

The upper histogram is real data, the middle one is data from $K_S \rightarrow \mu^+\mu^-\gamma$ Montecarlo, and the last is $K_L \rightarrow \mu^+\mu^-\gamma$ Montecarlo

5.7 Ratio of $\mu^+\mu^-\gamma$ and $\mu^+\mu^-$ Transversal Momentum

Our reaction is a kaon decaying into two photons, one of them virtual, that goes into a pair of muons. If we build the transversal momentum of the three decay products the expected value should be small. However, if we build it only for the two muons pair, we are doing it for the virtual photon, which of course has a lot of transversal momentum.

So, the ratio $\frac{P_T(\mu\mu\gamma)}{P_T(\mu\mu)}$ should be very small, as we see in the figure 7 this cut is very effective. It removes mainly decays which do not come from the type $K \rightarrow \gamma\gamma^*$, that is, decays whose photon come from bremmstralung (and it is usually emited in the same direction af the decay product) such as $K \rightarrow \pi^+\pi^-\gamma$.

Figure 7: RATIO $\frac{P_T(\mu\mu\gamma)}{P_T(\mu\mu)}$

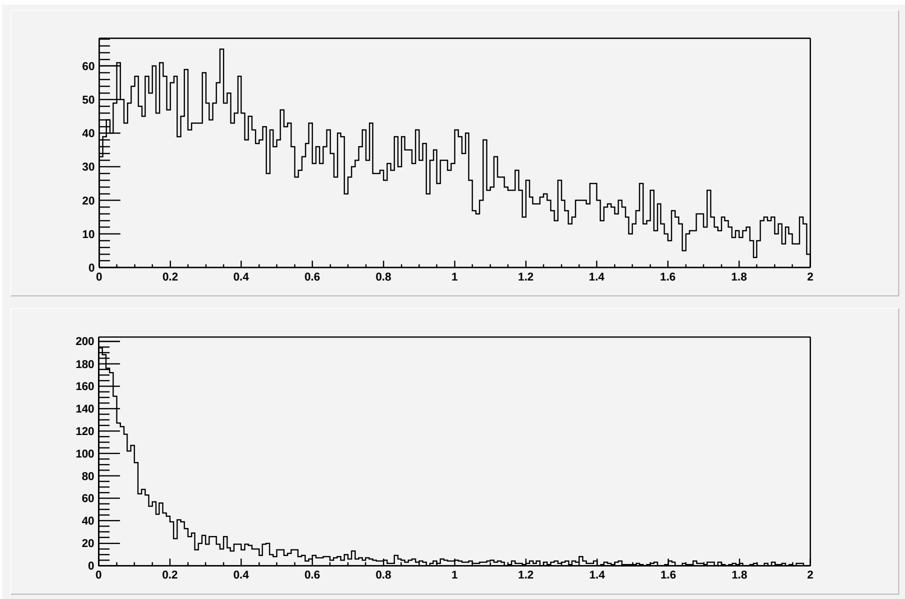

Upper histogram: real data (after cut in 10 GeV gamma energy). Lower histogram: $K_S \rightarrow \mu^+\mu^-\gamma$ Montecarlo

5.8 $\mu^+\mu^-\gamma$ Invariant Mass Cut

As we see in $K_S \to \mu^+\mu^-\gamma$ Montecarlo (figure 8) after all the cuts we should be able to build an invariant mass for our decay using the two tracks and the photon found. MC gives us a peak around 0.5 GeV, as we expected. That should be our final cut: build invariant masses for all the events that passed the filters and cut around the 0.5 GeV peak.

Figure 8: $K_S \to \mu^+\mu^-\gamma$ Invariant Mass

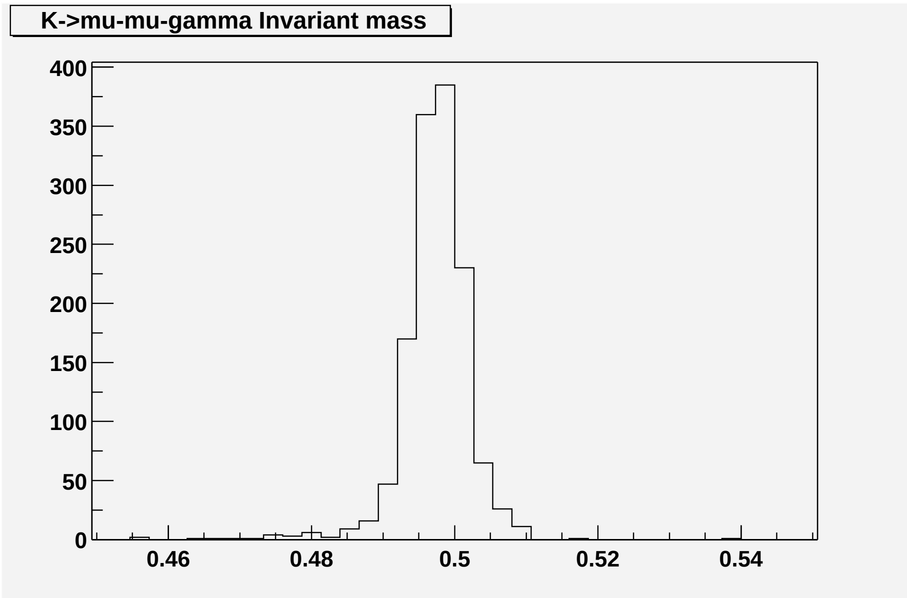

5.9 Other Cuts

We require that the Closest Distance of Aproach (CDA) of the reconstructed vertex must be less than 3 cm. We also require a number of tracks equal to two.

6 $K_S \to \mu^+\mu^-\gamma$ and $K_L \to \mu^+\mu^-\gamma$ Comparison

The decay $K_L \to \mu^+\mu^-\gamma$ has already been studied by NA48[4] and Fermilab[5] and satisfactory results were obtained. But our interest is in $K_S \to \mu^+\mu^-\gamma$, which in principle should have only the difference of the lifetime and the new decay channels.

However, during our analysis we found more differences derived from these two points. In previous studies of $K_L \to \mu^+\mu^-\gamma$ by NA48 another target placed much far away from the detector was used, thus eliminating all the K_S. In our analysis we use another target, much more nearer, and we have both K_S and K_L, with their particular background too.

One of the first effects we may note is that the decaying vertex position is strongly related with the energy of the decaying particle:

$$Z_{vertex} = \gamma\beta c\tau_S \approx E/m \times c\tau_S$$

Thus, the higher the energy of the particle, the greater the distance of decay. We already said that there was a 1 τ_S lenght collimator after the target, and all the particles that decay inside it have very few probabilities of being detected, because they hit the collimator walls from *inside*. That is not such a big problem for K_L, which has such a long lifetime compared with the collimator lenght , but it is important for K_S, because only the most energetic kaons will decay after the collimator, and then be seen. In table 9 can be seen this effect. In principle we should have a nice exponential, but we see no events before one lifetime, then it increases (these are the decays inside the collimator [9]) and after the collimator we have the typical exponential of decay.

This is the first difference in this analysis: *the greater energy of the decaying particle*. Every energy related measure will increase proporcionally with it: the transversal momentum, the momenta of the tracks, the energy of the photons (see figure 6)...

Also, to reconstruct the direction of the kaon we need the vertex of decay and the target position, but as they are very near to each other, that direction cannot be well stablished. That *resolution effect*, combined with the greater energy will lead to less efficiency of transversal momentum and ratio[10] cuts.

[9] Of which only some decay in the collimator direction and then are seen

[10] That is $\frac{P_T(\mu\mu\gamma)}{P_T(\mu\mu)}$ Ratio if anything else said

Figure 9: Position of Decay Vertex in Units of τ_S

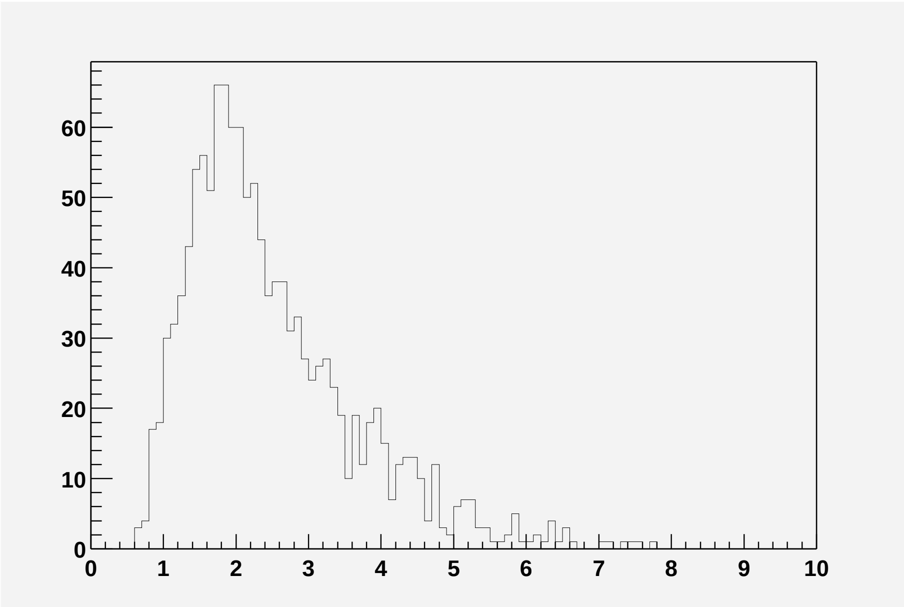

In figure 10 we can see the much greater dispersion of these two variables for the K_S than for the K_L. That can also be seen in figures 11 and 12.

In table 5 we can observe how our acceptance falls because of these effects. It can be seen to that K_L is a little more sensible to increase in gamma energy cuts that K_S (as we expected).

Table 5: Acceptances and Cuts Made

$P_T <$	$(Ratio)^2 <$	*Gamma Energy* $<$	K_S MC	K_L MC
$\sqrt{0.002}$ GeV	0.03	8 GeV Cuts made in [4]	5.52%	12.10%
0.2 GeV	0.1	10 GeV	16.37%	20.99%
0.3 GeV	0.2	10 GeV	23.11%	22.76%
0.2 GeV	0.1	15 GeV	15.05%	17.58%
0.3 GeV	0.2	15 GeV	21.54%	19.22%

Figure 10: Transversal Momentum Vs. Ratio Dispersion Diagram

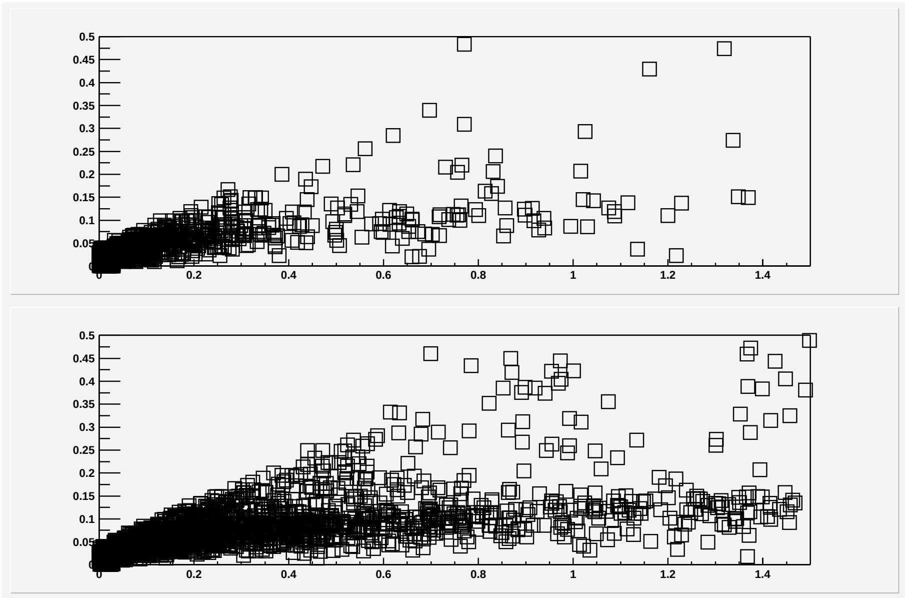

Upper diagram: Montecarlo for K_L. Lower diagram: K_S Montecarlo

7 Conclusion

Although we have not been able to see a peak in the invariant mass diagram (see figure 13 as an example of histogram) several conclusions can be taken:

- There is still no implemented Muon-Vecto for Montecarlo analysis.
- The analysis is much more difficult than for $K_L \to \mu^+\mu^-\gamma$.
- Doubts with the muon-veto.

References

[1] Cristenson *et al*, Phys. Rev. Lett. 13, 138, 1964

Figure 11: COMPARISON OF TRANSVERSAL MOMENTUM

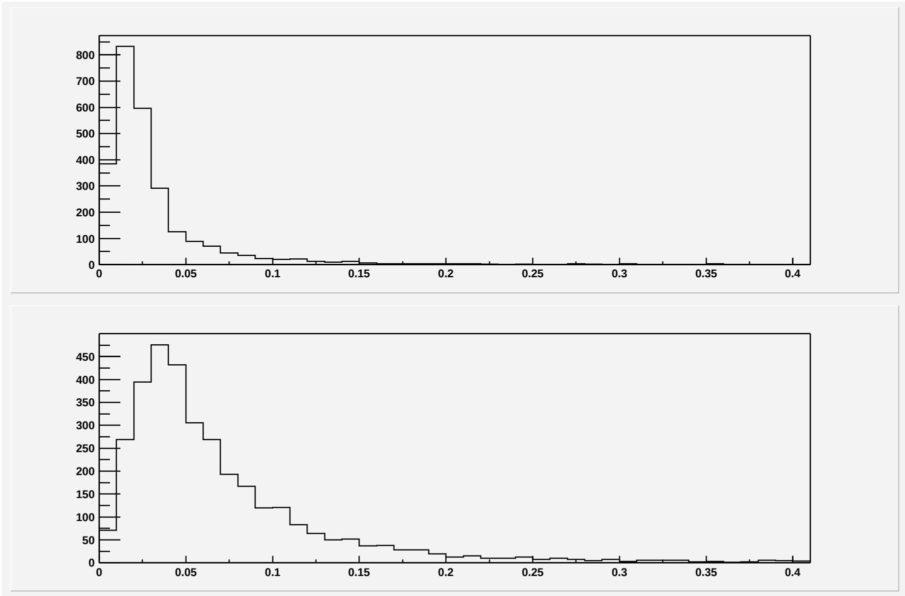

Upper histogram: Montecarlo for K_L. Lower histogram: K_S Montecarlo

[2] R. Batley *et al.*, *A high sensitivity investigation of K_S and neutral hyperon decays using a modified K_S beam (Addendum 2 to P253)*, CERN/SPSC 2002-002, 1999

[3] V. Fanti *et al.*, *Measurement of the decay rate and form factor parameter alpha(K*) in the decay $K_L \to e^+e^-\gamma$*, Phys. Lett. B, 458:553-563, 1999

[4] J. Scheidt, *Messung des Zerfalls $K_L \to \mu^+\mu^-\gamma$*, Johannes Gutenberg Universität, Mainz, 1996

[5] G. Breese, *A measurement of the branching ratio and form factor of $K_L \to \mu^+\mu^-\gamma$*, University of Chicago, 2000

Figure 12: Comparison of Ratio

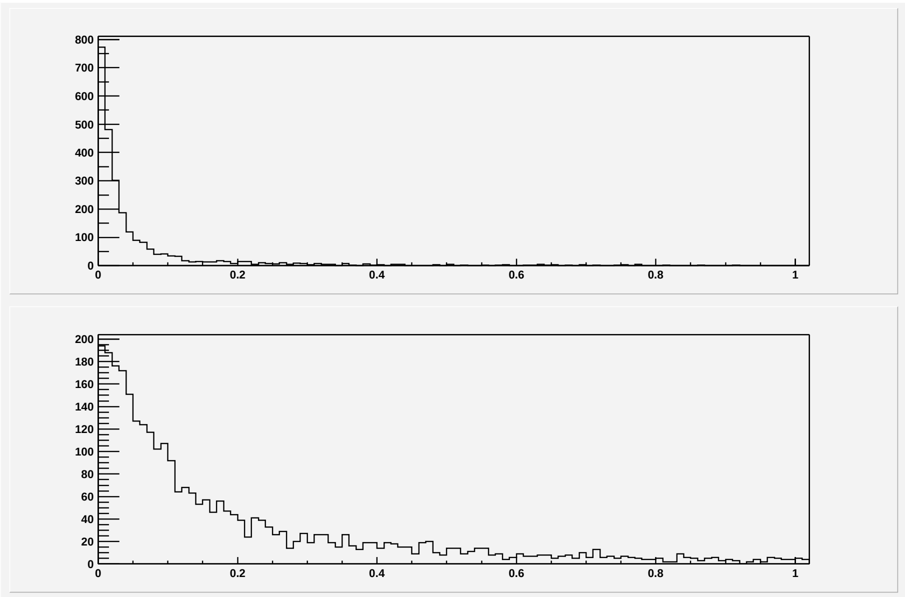

Upper histogram: Montecarlo for K_L. Lower histogram: K_S Montecarlo

Figure 13: Example of Invariant Mass Diagram

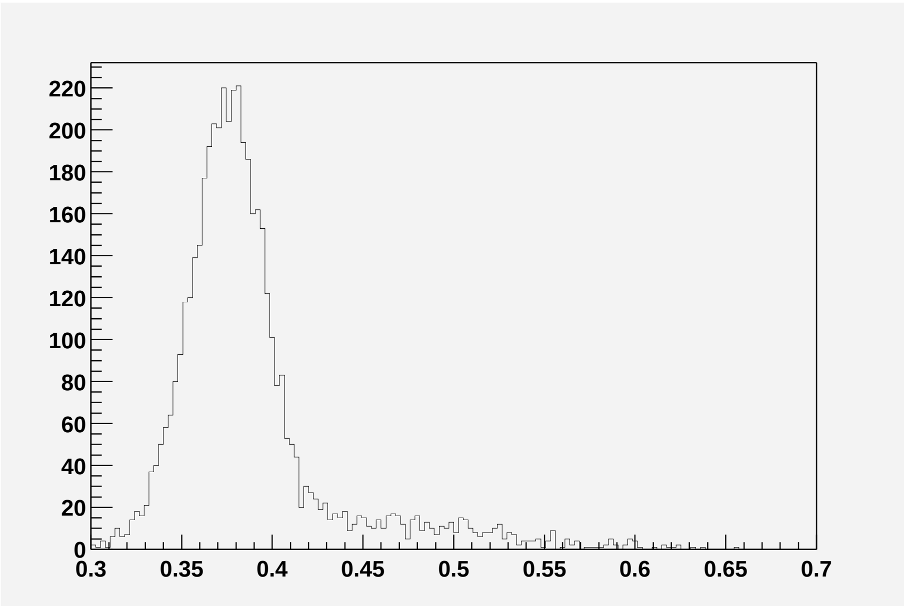

The peak around 0.35 GeV belongs to $K_L \to \pi^+\pi^-\pi^0$ events. We would expect a peak at 0.5 GeV but nothing is seen